RSC Advances

ROYAL SOCIETY OF CHEMISTRY

www.rsc.org/advances

Cite this: DOI: 10.1039/c0xx00000x

www.rsc.org/xxxxxx

ARTICLE TYPE

Al^{3+} selective coumarin based reversible chemosensor: application in living cell imaging and as integrated molecular logic gate

Deblina Sarkar,[a] Arindam Pramanik,[b] Sujan Biswas,[a] Parimal Karmakar[b] and Tapan Kumar Mondal[a]*

Received (in XXX, XXX) XthXXXXXXXXX 20XX, Accepted Xth XXXXXXXXX 20XX

DOI: 10.1039/b000000x

An efficient coumarin based fluorescent 'turn-on' receptor (H_2L) for the detection of Al^{3+} has been synthesized following simple Schiff base condensation of 4-Hydroxy-3-acetylcoumarin with 2-Amino-4-methylphenol. The receptor H_2L shows about 21 fold increase in fluorescent intensity upon addition of Al^{3+} than in case of other metals. The limit of detection is 0.39 μM. H_2L is efficient in detecting Al^{3+} in intracellular region of human cervical cancer cell and also exhibits an INHIBIT logic gate with Al^{3+} and EDTA as chemical inputs by monitoring both the absorption as well as emission mode. Theoretical calculations (DFT and TDDFT) are applied to interpret the sensing mechanism of the synthesized receptor.

Introduction

Aluminium being the third most abundant element in the earth's crust[1] has tremendous utility in the field of food packaging industries, electrical industries, food processing, water purification and clinical drugs etc.[2] However free Al^{3+} formed from leaching due to acid rain can be a fatal to growing plants.[3] Al^{3+} has neurotoxic activities[4] and been identified as a major cause of Alzheimer's disease[5] and Parkinson's disease.[6] Moreover Al^{3+} is also biologically very toxic causing osteomalacia, breast cancer and also intoxication in haemodialysis patients.[7] According to WHO, the permissible weekly intake of Al^{3+} should not exceed 7 mg Kg^{-1} body weight.[8] Thus detection of Al^{3+} in environmental and biological samples have gained a lot of importance.[9] Among the several detection techniques of Al^{3+},[10] fluorescence technique is popularly used due to its simplicity in operation, high sensitivity, rapidity and non-destructive nature.[11] Till date, various 'turn-on' fluorescent chemosensors have been reported where the basis fluorophore used are hydrazone, pyrollidine, 8-Hydroxyquinoline, oxazoline, imidazoline etc.[12] Recently, Goswami*et al*. reported a molecular switch for Al^{3+} based on spiropyran platform.[13] Very few Al^{3+} sensor based on coumarin framework has been reported so far but most of them suffer from the problem of cost of starting material, irreversibility, low limit of detection.[14] However in our present work we report herein a coumarin based chemosensor for the detection of Al^{3+} which has excellent selectivity, very low limit of detection and can be synthesized easily using a very economically cheap route. On top of that the developed sensor is reversible i,e, in presence of EDTA the receptor (H_2L) gets completely free from H_2L-Al^{3+} complex and hence can be used over again. Gradual addition of Al^{3+} (10 μM) to the receptor H_2L (10 μM) in MeOH/H_2O, 1:1, v/v (at 25°C) shows an excellent fluorescence emission intensity enhancement of 21 fold. Again H_2L represents an INHIBIT logic gate with Al^{3+} and EDTA as inputs through both the absorption and emission mode.[15] The receptor H_2L can also act as Al^{3+} sensor in living cells. Further theoretical calculation using DFT/B3LYP method has been used to interpret the sensing mechanism as well as electronic structure of the synthesized receptor H_2L.

Results and discussion

Synthesis and spectral characterisation

Synthetic route towards H_2L involves a very facile andeconomically cheap route using Schiff base condensation of 3-acetyl-4-hydroxycoumarin with 2-Amino-4-methylphenol in 1:1 molar ratio in methanolic medium under refluxing condition (Scheme 1).

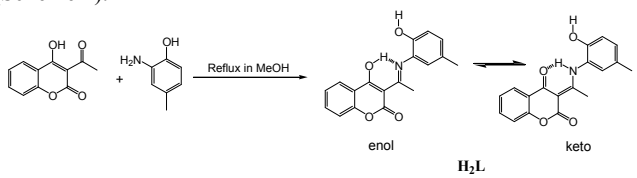

H_2L

Scheme 1. Synthesis and keto-enoltautomerism of chemosensor H_2L

IR spectrum taken in KBr disk shows stretching at 1710 cm^{-1} corresponding to lactone C=O, the keto C=O and C=C appears at 1619 cm^{-1} and 1571cm^{-1} respectively. ^{1}HNMR spectra are recorded in $CDCl_3$ which shows band at around δ 15.43 which is due to the hydrogen bonded NH proton (Fig. S1). This peak vanishes in the H_2L-Al^{3+} complex indicating co-ordination to the metal centre through N donating site in the enol form. The aromatic protons in H_2L appear as expected in the region δ 8.06-6.90. The –OH proton appears as a singlet at δ 5.95. The –

$COCH_3$ protons appear at δ 2.65 as singlet and the Ph-CH_3appear at δ 2.32. In the H_2L-Al^{3+} complex the –OH peak also vanishes indicating co-ordination to Al^{3+} using O centre (Fig. S1). All aromatic protons appear at a bit downfield position compared to that of H_2L, which can be clearly explained due to the co-ordination of Al^{3+} with H_2L. Mass spectrum shows m/z peak corresponding to $Na^+[H_2L]$ at 332.1 along with a peak at 310.1 corresponding to $H^+[H_2L]$ for H_2L (Fig. S2). For H_2L-Al^{3+} complex the strong peak at 419.3 correspond to $Na[Al(L-2H)NO_3]^+$ along with a weak peak at 437.3 corresponding to $Na^+[Al(L-2H)(NO_3)(H_2O)]$ species (Fig. S3) supporting 1:1 complex formation.

Cation sensing studies of H_2L

UV-Vis study

Receptor H_2L (10 μM) shows a strong absorbance band at 326 nm, in 1:1, v/v MeOH:H_2O using HEPES buffered solution at pH=7.2. Gradual addition of Al^{3+} (10 μM) shows a slight red shift of this band to 330 nm and a new band appears at 414 nm. Distinct isosbestic point appears at 369 nm (Fig. 1). This formation of new band at 414 nm indicates the co-ordination of the receptor to Al^{3+}. Interestingly when to this solution 10 μM EDTA solution is gradually added the band at 414 nm again gets depressed with the formation of new band at 326 nm (Fig. 2). This clearly indicates that the synthesized receptor H_2L shows reversibility in binding with Al^{3+}. In presence of EDTA, Al^{3+} gets free from the receptor, thus it can again be used for the detection of Al^{3+}. UV-Vis spectrum of H_2L is also studied in presence of other metals i,e, Na^+, K^+, Ca^{2+}, Mg^{2+}, Mn^{2+}, Fe^{3+}, Cr^{3+}, Co^{2+}, Ni^{2+}, Cu^{2+}, Cd^{2+} and Hg^{2+} but no significant changes are observed except for Zn^{2+} and Cu^{2+} (Fig. S4). The change in colour of H_2L in presence of Al^{3+} compared to other metals is also visible under naked eye (Fig. S5).

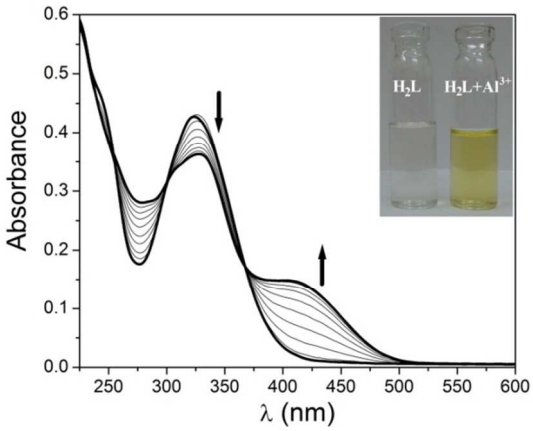

Fig. 1. Change in UV-Vis spectrum of H_2L (10 μM) upon gradual addition of 10 μM Al^{3+} in 1:1, v/v MeOH:H_2O. Inset shows the visual effect of addition of Al^{3+} to H_2L in ambient light.

Fluorescence study

In the absence of metal ions the emission spectrum of the synthesized chemosensor H_2L shows a very weak emission band with maxima (F_0) at 371 nm ($\lambda_{excitation}$, 326 nm). The fluorescence quantum yield (ϕ = 0.006) is very poor. Gradual addition of Al^{3+} to the above solution shows an excellent fluorescence enhancement by 21 fold (ϕ = 0.076) and the maxima at 371 nm vanished with the formation of new emission maxima at 398 nm (Fig. 3). This red shift of 27 nm is due to co-ordination of the metal centre to the receptor. This fluorescence enhancement reflects a strong selective OFF-ON fluorescent signaling property of H_2L for Al^{3+}. On addition of EDTA, fluorescent intensity at 398 nm gradually decreases (Fig. 4). This indicates the reversible nature of the receptor and thus our synthesized receptor can be used over and over again making it very economically useful. Thus H_2L basically shows an OFF-ON-OFF signally pattern in presence of Al^{3+} and EDTA.

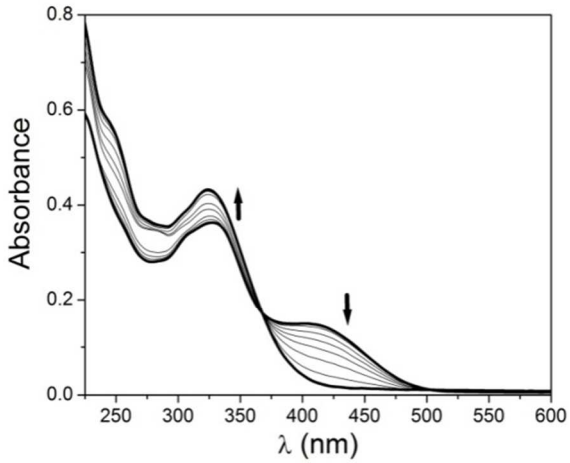

Fig. 2. Change in UV-Vis spectrum of H_2L-Al^{3+} (10 μM) upon gradual addition of EDTA (10 μM) in 1:1, v/v MeOH:H_2O

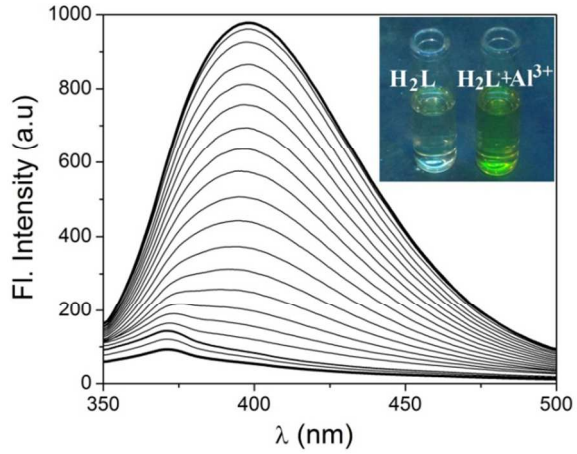

Fig. 3. Change in emission spectrum of H_2L (10 μM) upon gradual addition of 10 μM Al^{3+} 1:1, v/v MeOH:H_2O. Inset shows the visual effect of addition of Al^{3+} to H_2L under UV light.

Jobs plot of emission intensity shows a maxima in the plot corresponds to ~0.5 mole fraction indicating 1:1 complex formation of H_2L with Al^{3+} (Fig. S6). From emission spectral change, limit of detection of the chemosensor for Al^{3+} is determined using the equation LOD= K × SD/S where SD is the standard deviation of the blank solution and S in the slope of the calibration curve (Fig. S7). The limit of detection for Al^{3+} is 0.393μM from fluorescent spectral titration. This result clearly

demonstrates that the chemosensor is highly efficient in sensing Al^{3+} even in very minute level. From fluorescent spectral titration the association constant of H_2L with Al^{3+} is found to be 4.8×10^5 and stoichiometry of the reaction n = 1.17 indicating 1:1 complex formation (Fig. S8).

Fluorescence emission intensity of H_2L (10 μM) is studied in presence of other metals i,e, Na^+, K^+, Ca^{2+}, Mg^{2+}, Mn^{2+}, Fe^{3+}, Cr^{3+}, Co^{2+}, Ni^{2+}, Cu^{2+}, Cd^{2+} and Hg^{2+} (10 μM) in MeOH:H_2O (1:1, v/v, pH=7.2) but there is hardly any increase in emission intensity of H_2L (Fig. 5). Then to these solutions Al^{3+} is added which then shows an obvious fluorescent enhancement (Fig. S9). Thus the synthesized receptor H_2L is highly efficient in detection of Al^{3+}even in presence of other metals and thus it can detect Al^{3+} in biological or environmental samples where other metals usually co-exist with Al^{3+}.

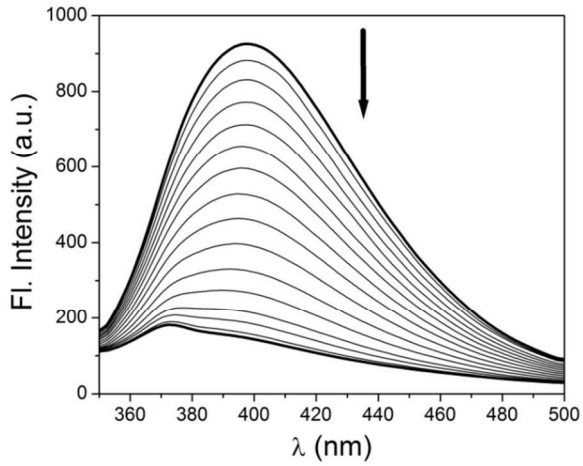

Fig. 4. Change in emission spectrum of H_2L-Al^{3+} (10 μM) upon gradual addition of EDTA (10 μM) in 1:1, v/v MeOH:H_2O

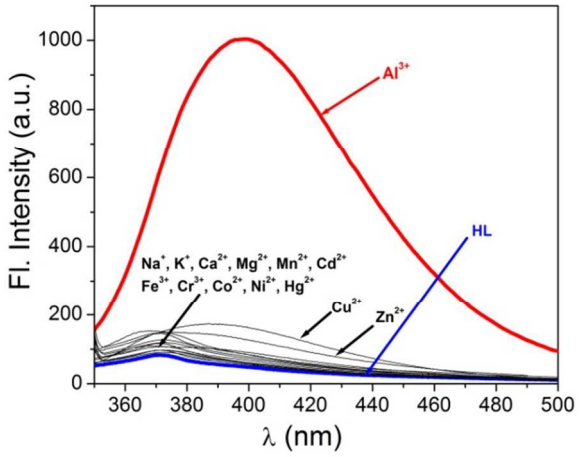

Fig. 5. Change in emission spectrum of H_2L (10 μM) upon addition of Na^+, K^+, Ca^{2+}, Mg^{2+}, Mn^{2+}, Fe^{3+}, Cr^{3+}, Al^{3+}, Co^{2+}, Ni^{2+}, Cu^{2+}, Cd^{2+} and Hg^{2+} (10 μM) in MeOH: H_2O (1:1, v/v, pH=7.2).

The effect of pH on the emission intensity of the receptor (H_2L) in absense and presence of Al^{3+} is studied. In case of H_2L there is hardly any change in fluorescence intensity in the pH range 5-10 (Fig. 6). Below pH 5 sharp increase in fluorescence intensity is observed due to protonation of imine N and hydroxy O atoms preventing the excited state intramolecular proton transfer (ESIPT) process, which is responsible for the quenching of fluorescence intensity.[16] On addition of 1.2 equivalents of Al^{3+} the fluorescence intensity remains almost unchanged in the pH < 4, while there is a sharp increase in fluorescence intensity in the pH range 5-8. But, on further increase in pH fluorescence intensity drops drastically due to the formtion of $Al(OH)_3$ at pH > 8. Thus the receptor (H_2L) is efficient in detection of Al^{3+} in the biologically relevant pH range (6.0-7). However at low pH values (pH < 4) receptor tends to combine with protons and hence becomes ineffective in detection of Al^{3+}.

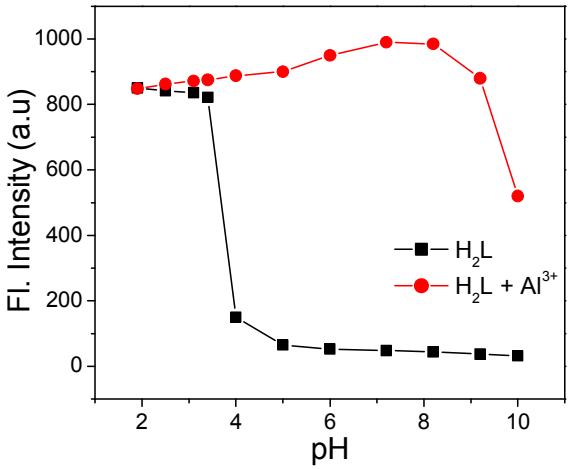

Fig. 6. pH dependence of fluorescence intensity of H_2L and its complex with Al^{3+}.

Electronic structure and sensing mechanism

To interpret the electronic structure of H_2L geometry optimization has been performed by DFT/B3LYP method in singlet ground state (S_0) and first excited state (S_1) by TDDFT/B3LYP method. The potential energy scans (Fig. S10) in S_0 state revels that the keto form is more stable by an amount of energy of 7.308 kcal/mol than the corresponding enol form which is consistent with the X-ray structure of this type of molecules.[17] The geometry of H_2L-Al^{3+} has been optimized and the energy minimized structures are shown in Fig. 7. In the complex the chemosensor H_2L binds to Al^{3+} through two phenolic-O atoms and imine-N. In an octahedral geometric environment other three coordination site are satisfied by NO_3^- and two water molecules and the proposed geometry is supported by mass spectral analysis of H_2L-Al^{3+} complex. Contour plot of selected molecular orbitals of H_2L and its complex with Al^{3+} are given in Fig. S11 and Fig. S12 respectively. The HOMO-LUMO gap of H_2L is significantly decreased from 4.17 eV to 2.82 eV in Al^{3+}complex.

To interpret the changes in electronic spectra TDDFT calculation by DFT/B3LYP method has been carried out in MeOH. The intense band at 326 nm for chemosensor H_2L corresponds to HOMO → LUMO transition (Table 1). The new band at 414 nm along with peak at 330 nm for Al^{3+} complex are correspond to HOMO → LUMO and HOMO-1 → LUMO transitions respectively.

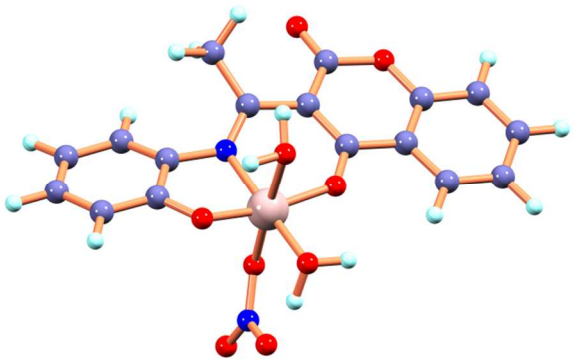

Fig. 7. Optimized structure of H_2L-Al^{3+} complex in DFT/B3LYP/6-311G(d) method

Table 1. Vertical electronic transitions calculated by TDDFT/CPCM method and experimental λ_{max} (nm)

Compds.	Excitation	$\lambda_{excitation}$ (nm)	Oscillator strength (f)	$\lambda_{expt.}$ (nm)
H_2L	HOMO → LUMO	353	0.3188	326
H_2L-Al^{3+}	HOMO → LUMO	430	0.3151	414
	HOMO-1 → LUMO	343	0.3139	330

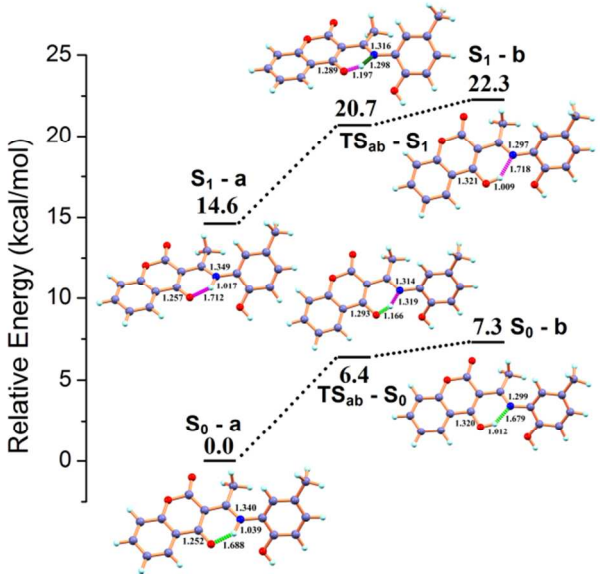

Fig. 8. The hydrogen transfer processes for H_2L in ground (S_0) and excited state (S_1), along with key bond lengths (Å) and relative energies (kcal/mol) at the DFT/B3LYP/6-311G(d) for the S_0 and TDDFT/B3LYP/6-311G(d) for S_1 state.

In the absence of Al^{3+}, H_2L shows a weak emmision band centered around 371 nm. Upon gradual addition of Al^{3+}, the receptor H_2L shows an excellent fluorescence intensity enhancement of 21 fold and a new emission band appears at 398 nm. To interprete whether the excited state intramolecular proton transfer (ESIPT)[16] is responsible for the quenching of fluorescence intensity for H_2L, theoretical calculastions are carried out. The possible intramolecular proton transfer process both in ground (S_0) and excited (S_1) state have been considered (Fig. 8). The energy difference between S_0 and S_1 states is only 14.63 kcal/mol and the hydrogen transfer can proceed very easily both in ground and excited state with a energy barrier of 6.42 and 6.10 kcal/mol respectively. Thus DFT calculations suggest that H_2L exists in the form of S_0-a and S_1-a in the ground- and excited state respectively. The hydrogen transfer takes place easily both in ground and excited state resulting in quenching of fluorescence for H_2L. On coordination with Al^{3+} this ESIPT process is inhibited resulting in fluorescence intensity enhancement.

Application as Logic function

Arithmatic operations performed by several combination of logic gates are widely implimented in semiconductor technology [18] as well as for computation in nano scale level.[19] Several molecular function systems[20] are reported recently. Now molecular logic function was studied with our synthesized chemosensor H_2L along with Al^{3+} as well as the chelating agent EDTA as inputs. As discussed earlier absorption band at 414 nm emerged in presence of Al^{3+} and again in presence of EDTA the absorption band at 414 nm decreased along with decrease in emission band at 398 nm. Thus with two inputs as Al^{3+} and EDTA, H_2L has the ability to exhibit INHIBIT function via both absoption as well as emission output. Only when Al^{3+} is present the absorption as well as emission at 414 nm and 398 nm respectively is 1 while the values of all other functions are 0. Actually it represents an AND gate with an inverter[21] in one of its input. Thus the absorption change at 414 nm and emission change at 398 nm with Al^{3+} as well as EDTA as inputs can be interpretated as a monomolecular circuit showing an INHIBIT logic function (Fig. 9).

Input		Output	
IN1	IN2	OUT1	OUT2
Al^{3+}	EDTA	Absorption at 414 nm	Emission at 398 nm
0	0	0	0
0	1	0	0
1	0	1	1
1	1	0	0

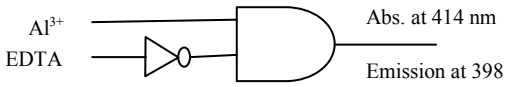

Fig. 9. Truth table and the monomolecular circuit based on Al^{3+} and EDTA

Biological Application Study

To explore the biological application of the synthesized receptor H_2L, Human cancer cell line HeLa are treated with the receptor and receptor -Al^{3+} complex separately for 24 h. The cells are able to take up both the receptor as well as Al^{3+}. The cells treated with

ligand at a dose of 10 μM have a slight green fluorescence at a range of 370 nm. This clearly indicates that the receptor has some autofluorogenic properties when applied to biological systems. Upon addition of equimolar Al^{3+} (10 μM), increase in intensity of fluorescence emission is observed (Fig. 10). Thus the synthesized receptor H_2L has the potential for live cell imaging and can be used in detection of Al^{3+} in the intracellular region.

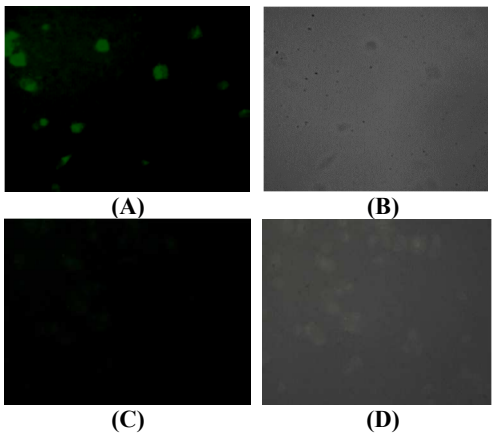

Fig. 10. (A) Fluorescence image of HeLa cells after incubation with 10 μM Al^{3+} and 10 μM H_2L and respective brightfield (B). (C) Flourescence image of HeLa cells after incubation with 10 μM H_2L and its respective bright field (D).

HeLa cells are treated with Al^{3+}, H_2L and H_2L-Al^{3+} complex at various concentrations (5 μM – 80 μM). But it is observed that H_2L has slight effect on survivability of cells at higher dosage (40 μM) (Fig.11).

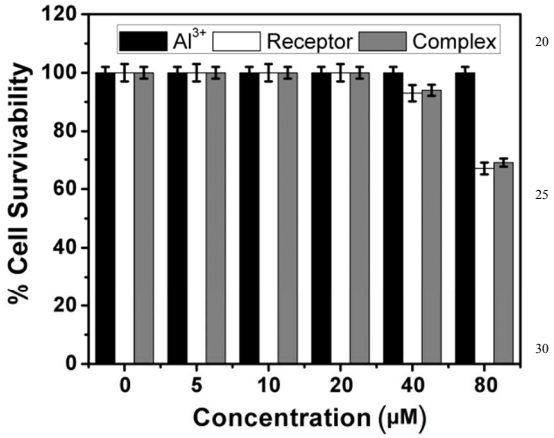

Fig. 11. MTT assay of Al^{3+}, H_2L and H_2L-Al^{3+} complex on HeLa cells. ($p>0.05$ as compared with respective controls).

Experimental

Material and methods

4-Hydroxycoumarin and 2-Amino-4-methylphenol were purchased from Aldrich. All other organic chemicals and inorganic salts were available from commercial suppliers and used without further purification.

Elemental analysis was carried out in a 2400 Series-II CHN analyzer, Perkin Elmer, USA. HRMS mass spectra were recorded on Waters (Xevo G2 Q-TOF) mass spectrometer. Infrared spectra were taken on a RX-1 Perkin Elmer spectrophotometer with samples prepared as KBr pellets. Electronic spectral studies were performed on a Perkin Elmer Lambda 25 spectrophotometer. Luminescence property was measured using Perkin Elmer LS 55 fluorescence spectrophotometer at room temperature (298 K). NMR spectra were recorded using a Bruker (AC) 300 MHz FTNMR spectrometer in $CDCl_3$.

The luminescence quantum yield was determined using carbazole as reference with a known ϕ_R of 0.42 in MeCN. The complex and the reference dye were excited at the same wavelength, maintaining nearly equal absorbance (~0.1), and the emission spectra were recorded. The area of the emission spectrum was integrated using the software available in the instrument and the quantum yield is calculated according to the following equation:

$$\phi_S/\phi_R = [A_S / A_R] \times [(Abs)_R /(Abs)_S] \times [\eta_S^2/\eta_R^2].$$

Here, ϕ_S and ϕ_R are the luminescence quantum yield of the sample and reference, respectively. A_S and A_R are the area under the emission spectra of the sample and the reference respectively, $(Abs)_S$ and $(Abs)_R$ are the respective optical densities of the sample and the reference solution at the wavelength of excitation, and η_S and η_R are the values of refractive index for the respective solvent used for the sample and reference.

Synthesis of 3-(1-(2-hydroxy-5-methylphenylimino) ethyl)-4-hydroxy-2H-chromen-2-one (H_2L)

3-Acetyl-4-hydroxy-2H-chromen-2-one (L)[22] (0.184 g, 0.9 mmol)and 2-Amino-4-methylphenol (0.111 g, 0.9 mmol) were refluxed for 6 hours in methanolic medium. Excess solvent was evaporated under reduced pressure and then dissolved in dichoromethane which is then further subjected to silica gel (60-120 mesh) column chromatographic separation. The desired light yellow solid product was obtained by elution with 20% ethylacetate:petether (v/v) mixture. Yield was, 0.243 g, 88%.

Anal. Calc. for $C_{18}H_{15}NO_4$ (H_2L): Calc. (%) C 6.89, H 4.89, N 4.53. Found (%), C 6.97, H 4.91, N 4.51. IR data (KBr, cm^{-1}): 1710 υ(lactone C=O); 1619 υ(keto C=O), 1571 υ(C=C). ^1H NMR data ($CDCl_3$, 300 MHz): δ 15.44 (1H, s), 8.05 (1H, d, J = 7.5 Hz), 7.57 (1H, t, J= 7.1 Hz), 7.24-7.21 (2H, m), 7.09(1H, d, J = 8.27 Hz), 6.94-6.90 (2H, m), 5.95 (1H, s), 2.65 (3H, s), 2.51 (3H, s).

General method for UV-Vis and fluorescence titration

Stock solution of the receptor H_2L (10 μM) in [(MeOH/H_2O), 1:1, v/v] (at 25°C) using HEPES buffered solution at pH = 7.2 was prepared. The solution of the guest cations using their chloride salts in the order of 100 μM were prepared in deionized water. Solutions of various concentrations containing host and increasing concentrations of cations were prepared separately. The spectra of these solutions were recorded by means of UV-Vis methods. EDTA solution of 100 μM was added to the same solution where Al^{3+} was added gradually to H_2L and UV spectra recorded. The spectra of all these solutions were also recorded by means of fluorescence methods.

Job's plot by fluorescence method

A series of solutions containing H_2L (10 μM) and $Al(NO_3)_3$ (10 μM) were prepared in such a manner that the sum of the total metal ion and H_2L volume remained constant (4 mL). MeOH:H_2O (1:1, v/v) was used as solvent at pH 7.2 using HEPES buffer. Job's plots were drawn by plotting ΔF versus mole fraction of Al^{3+} [ΔF = change of intensity of the emission spectrum at 398 nm (for Al^{3+}) during titration and X_g is the mole fraction of the guest in each case].

In vitro cell imaging

Cell Cytotoxicity assay: HeLa cells were evaluated for cytotoxicity with aluminium nitrate (Al^{3+}), H_2L and H_2L-Al^{3+} complex by the following protocol as described by Shi et al (2012).[23] Cells were seeded in 96-well plates at a density of 1×10^4 cells per well and cultured for 24 h. Al^{3+} was treated in aqueous medium while ligand was dissolved in DMSO but final concentration of DMSO while treatment of cells was maintained below 1%. After treatment for 24 h, Methyl tetrazolium dye (MTT) was used to determine the cell viability and absorbance of MTT formazan was determined at 595 nm in spectrophotometer (Epoch Micro-plate Spectrophotometer, USA). Untreated cells were served as 100% viable.

Cell Bio-imaging: HeLa cells were seeded for overnight. Further cells were treated with ligand and complex respectively for 45 mins at a dose less than LD_{50} (10 μM). After treatment cells were washed with 1X Phosphate buffer saline and observed under fluorescent microscope at excitation of 326 nm and bright field.

Data analysis: We repeated these experiments six times and the data were expressed by calculating the standard deviation of all the six experiments. Comparisons of the mean of experiments were made by a model I ANOVA test (using a statistical package, Origin 6, Northampton, MA) with multiple comparisont-tests, $p>0.05$ as a limit of significance.

Computational method

All calculations were carried out at the B3LYP[24] level using Gaussian 09 software.[25] The 6-311G(d) basis set was assigned for the elements. All the ground state (S_0) stationary points were fully optimized at the B3LYP/6-311G(d) and the excited states at TD-B3LYP/6-311G(d) method.[26,27] Vertical electronic excitations based on B3LYP optimized geometries were computed using the time-dependent density functional theory (TDDFT) formalism[28] in methanolusing conductor-like polarizable continuum model (CPCM).[29]

Conclusions

Thus we have successfully developed a new coumarin based reversible chemosensor for the selective detection of Al^{3+} over other metal ions. Fluorescence intensity enhancement of 21 fold upon addition of 10 μM Al^{3+} to H_2L (10 μM) is observed. More importantly the developed chemosensor can also detect Al^{3+} in the intracellular region of human cervical cancer cells. H_2L can also function as an INHIBIT logic gate with Al^{3+} and EDTA as inputs.

Acknowledgement

Financial supports received from the Department of Science and Technology, New Delhi, India is gratefully acknowledged. D. Sarkaris thankful to CSIR, New Delhi, India, S. Biswas is thankful to UGC, New Delhi for fellowship. A. Pramanik is thankful to DBT, India for his fellowship.

Notes and references

[a]*Department of Chemistry, Jadavpur University, Kolkata-700032, India E-mail: tkmondal@chemistry.jdvu.ac.in*
[b]*Department of Life Science and Biotechnology, Jadavpur University, Kolkata-700 032,*
E-mail: pkarmakar_28@yahoo.co.in (P. Karmakar).
†Electronic Supplementary Information (ESI) available: [Association constant determination, detection limit determination, ^{1}H NMR, HRMS, UV-Vis titration spectra of HL with different metal ions etc.]. See DOI: 10.1039/b000000x

1 W. S. Miller, L. Zhuang, J. Bottema, A. J. Wittebrood, P. De Smet, A. Haszler and A. Vieregge, *Mater. Sci. Eng., A*, 2000, **280**, 37; R. E. Doherty, *Environ. Forensics*, 2000, **1**, 83; G. Ciardelli and N. Ranieri, *Water Res.*, 2001, **35**, 567.
2 M. G. Sont, S. M. White, W. G. Flamm and G. A. Burdock, *Regul. Toxicol. Pharmacol.*, 2001, **33**, 66; N. W. Bavlor, W. Egan and P. Richman, *Vaccine*, 2002, **20**, S18; J. Exley, *Inorg. Biochem.*, 2005, **99**, 1747.
3 E. Delhaize and P. R. Ryan, *Plant Physiol.*, 1995, **107**, 315.
4 D. R. Crapper McLachlan, W. J. Lukiw and T. P. A. Kruck, *Environ. Geochem. Health*, 1990, **12**, 103.
5 T. P. Flaten, *Brain Res. Bull.*, 2001, **55**, 187; J. R. Walton, *Curr. Inorg. Chem.*, 2012, **2**, 19.
6 J. R. Walton, *NeuroToxicology*, 2006, **27**, 385.
7 G. C. Woodson, *Bone*, 1998, **22**, 695; P. D. Darbre, *J. Inorg. Biochem.*, 2005, **99**, 1912; G. D. Fasman, *Coord. Chem. Rev.*, 1996, **149**, 125.
8 B. Valeur, I. Leray, *Coord. Chem. Rev.*, 2000, **205**, 3.
9 Y. Kawanishi, K. Kikuchi, H. Takakusa, S. Mizukami, Y. Urano, T. Higuchi and T. Nagano, *Angew. Chem., Int. Ed.*, 2000, **112**, 3580; S. Deo, H. A. Godwin, *J. Am. Chem. Soc.*, 2000, **122**, 174; Z. Rengel and W. H. Zhang, *New Phytol.*, 2003, **159**, 295; E. Àlvarez, M. L. Fernández-Marcos, C. Monterroso, M. J. Fernández-Sanjurjo, *Forest Ecol. Manag.*, 2005, **211**, 227.
10 M. Ahmad, R. Narayanaswamy, *Talanta*, 1995, **42**, 1337; S. Saito, J.-I. Shimidzu, K. Yoshimoto, M. Maeda, M. Aoyama, *J. Chromatogr., A*, 2007, **1140**, 230; S. Murko, R. Milačič, J. Ščančar, *J. Inorg. Biochem.*, 2007, **101**, 1234.
11 D. T. Quang, J. S. Kim, *Chem. Rev.*, 2010, **110**, 6280; H. Kobayashi, M. Ogawa, R. Alford, P. L. Choyke, Y. Urano, *Chem. Rev.*, 2010, **110**, 2620.
12 M. P. Manuel-Vez and M. Garcia-Vargas, *Talanta*, 1994, **41**,1553; D. Maity and T. Govindaraju, *Chem. Commun.*, 2010, **46**, 4499; Y. Zhao, Z. Lin, H. Liao, C. Duan and Q. *Meng, Inorg. Chem. Commun.*, 2006, **9**, 966; A. Jeanson and V. Bereau, *Inorg. Chem. Commun.*, 2006, **9**,13; R. Patil, A. Moirangthem, R. Butcher, N. Singh,A. Basu, K. Tayade, U. Fegade,D. Hundiwale, A. Kuwar, *Dalton Trans.*, 2014, **43**, 2895.
13 S. Goswami, K. Aich, S. Das, A. K. Das,D. Sarkar, S. Panja, T. K. Mondal, S. Mukhopadhyay, *Chem. Commun.,* 2013, **49**, 10739.
14 M. Arduini, F. Felluga, F. Mancin, P. Rossi, P. Tecilla, U. Tonellato, N. Valentinuzzi, *Chem. Commun.*, 2003, 1606; S. Guha, S. Lohar, A. Sahana, A. Banerjee, D. A. Safin,M. G. Babashkina, M. P. Mitoraj, M. Bolte, Y. Garcia,S. K. Mukhopadhyay, D. Das, *Dalton Trans.*, 2013, **42**, 10198.
15 S. Wang, G. Men, L. Zhao, Q. Hou, S. Jiang, *Sens. Actuators, B*, 2010, **145**, 826.
16 A.J. Moghadam, R.Omidyan,. V. Mirkhani, . G. Azimi, *J. Phys. Chem. A*, 2013, **117**, 718; Z. Wang, D. M. Friedrich, C. C. Ainsworth,

S. L. Hemmer, A. G. Joly, M. R. Beversluis, *J. Phys. Chem. A*, 2001, **105**, 942; I. Presiado, Y. Erez, R. Gepshtein and D. Huppert, *J. Phys. Chem. C*,2010, **114**, 3634; F. Wua,, L. Ma , S. Zhanga, Y. Genga, J. Lüa, X. Chenga,*Chemical Physics Letters*, 2012, **519–520**, 141.

17 A. Brahmia, T.B. Ayed, R.B. Hassen, *Acta Crystallogr., Sect. E: Struct. Rep. Online*, 2013, **69**, o1296; T. Shibahara, M. Takahashi, A. Maekawa, H. Takagi, *Acta Crystallogr., Sect. E: Struct. Rep. Online*, 2010, **66**, o429.

18 M. L. P. Tan, H. C. Chin, L. L. Lim, , W. S. Wong, E. L. M. Su, C. F. Yeong, *Sci. Adv. Mater.,* 2014, **6**, 569; Y. Ha, K. Everaerts, M.C. Hersam, T.J.Marks, *Acc. Chem. Res.*, 2014, **47**, 1019.

19 G. Jiang, Y. Song, X. Guo, D. Zhang, D. Zhu, *Adv. Mater.*, 2008, **20**, 2888; S. K. Garai, *Opt Commun*, 2014, **313**, 441; J. Zhang, R. Laflamme, D. Suter, *Phys. Rev. Lett.*, 2012, **109**, 100503.

20 W. Zhou, J. Li, X. He, C. Li, J. Lv, Y. Li, S. Wang, H. Liu, D. Zhu, *Chem. Eur. J.*, 2008, **14**, 754; D. Zhang, Q. Zhang, J. Su, H. Tian, *Chem. Commun*. 2009, 1700; G. Zong, G. Lu, Acta Chim. Sin., 2009, **67**, 157.

21 A.P. de Silva, N.D. McClenaghan, *Chem. Eur. J*. 2002, **8**, 4935; M. Ikeda, T. Tanida, T. Yoshii, K. Kurotani, S. Onogi, K. Urayama, I. Hamachi, Nature Chemistry, 2014; Y. Fu, Q. Feng, X. Jiang, H. Xu, M. Li, S. Zang, Dalton Trans., 2014, **43**, 5815; D. C. Magri, M. C. Fava, C. J. Mallia, Chem. Commun., 2014, 50, 1009; S. Wang, G. Men, L. Zhao, Q. Hou, S. Jiang, *Sensors Actuat B-Chem*, 2010, **145**, 826.

22 N. Hamdi, C. Fischmeister, M.C. Puerta, P. Valerga, *Med. Chem. Res.*, 2011, **20**, 522.

23 L. Shi, C. Tang, C. Yin, *Biomaterials*, 2012, **33**, 7594.

24 A.D. Becke, *J. Chem. Phys.,* 1993, **98**, 5648; C. Lee, W. Yang, R. G. Parr, *Phys. Rev. B*, 1988, **37**, 785; D. Andrae, U. Haeussermann, M. Dolg, H. Stoll and H. Preuss, *Theor. Chim. Acta*, 1990,**77**, 123.

25 Gaussian 09, Revision D.01, M. J. Frisch, G. W. Trucks, H. B. Schlegel, G. E. Scuseria, M. A. Robb, J. R. Cheeseman, G. Scalmani, V. Barone, B. Mennucci, G. A. Petersson, H. Nakatsuji, M. Caricato, X. Li, H. P. Hratchian, A. F. Izmaylov, J. Bloino, G. Zheng, J. L. Sonnenberg, M. Hada, M. Ehara, K. Toyota, R. Fukuda, J. Hasegawa, M. Ishida, T. Nakajima, Y. Honda, O. Kitao, H. Nakai, T. Vreven, J. A. Montgomery, Jr., J. E. Peralta, F. Ogliaro, M. Bearpark, J. J. Heyd, E. Brothers, K. N. Kudin, V. N. Staroverov, R. Kobayashi, J. Normand, K. Raghavachari, A. Rendell, J. C. Burant, S. S. Iyengar, J. Tomasi, M. Cossi, N. Rega, J. M. Millam, M. Klene, J. E. Knox, J. B. Cross, V. Bakken, C. Adamo, J. Jaramillo, R. Gomperts, R. E. Stratmann, O. Yazyev, A. J. Austin, R. Cammi, C. Pomelli, J. W. Ochterski, R. L. Martin, K. Morokuma, V. G. Zakrzewski, G. A. Voth, P. Salvador, J. J. Dannenberg, S. Dapprich, A. D. Daniels, Ö. Farkas, J. B. Foresman, J. V. Ortiz, J. Cioslowski, and D. J. Fox, Gaussian, Inc., Wallingford CT, 2009.

26 F. Furche, R. Ahlrichs, *J. Chem. Phys*., 2002, **117**, 7433.

27 G. Scalmani, M. J. Frisch, B. Mennucci, J. Tomasi, R. Cammi and V. Barone, *J. Chem. Phys*., 2006, **124**, 1.

28 R. Bauernschmitt, R. Ahlrichs, *Chem. Phys. Lett*., 1996, **256**, 454; R.E. Stratmann, G.E. Scuseria, M.J. Frisch, *J. Chem. Phys*., 1998, **109**, 8218; M.E. Casida, C. Jamorski, K.C. Casida, D.R. Salahub, J. *Chem. Phys.,*1998, **108**, 4439.

29 V. Barone, M. Cossi, *J. Phys. Chem. A*, 1998, **102**, 1995; M. Cossi, V. Barone, *J. Chem. Phys.*, 2001, **115**, 4708; M. Cossi, N. Rega, G. Scalmani, V. Barone, *J. Comput. Chem.*, 2003, **24**, 669.

Abstract: An efficient coumarin based fluorescent 'turn-on' receptor (H_2L) for the detection of Al^{3+} has been synthesized. The receptor H_2L shows about 21 fold increase in fluorescent intensity upon addition of Al^{3+} than in case of other metals. The limit of detection is 0.39 μM. H_2L is efficient in detecting Al^{3+} in the intracellular region of HeLa cell and also exhibits an INHIBIT logic gate with Al^{3+} and EDTA as chemical inputs by monitoring both the absorption as well as emission mode. Theoretical calculations interpret the sensing mechanism of the synthesized receptor.